

Raman study of the CeO₂ texture as buffer layer in the CeO₂/La₂Zr₂O₇/Ni architecture for coated conductors

C. Jiménez¹, T. Caroff¹, A. Bartasyte¹, S. Margueron¹, A. Abrutis², O. Chaix-Pluchery¹, F. Weiss¹

1 LMGP – UMR 5628 CNRS – Grenoble INP –Minatec 3, parvis Louis Néel, BP 257 38016 Grenoble France

2 Departement of General and Inorganic Chemistry - Vilnius University - Naugarduko str.24, LT-03225 Vilnius - Lithuania.

Abstract

CeO₂/La₂Zr₂O₇/Ni piled-up structure is a very promising architecture for YBa₂Cu₃O₇ (YBCO) coated conductors. We have grown YBCO/CeO₂/LZO/Ni epitaxial structures by metalorganic decomposition (MOD) and metalorganic chemical vapour deposition (MOCVD) methods. The crystallographic quality of the CeO₂ layer is not well determined by conventional X-Ray Diffraction (XRD) due to the superposition of LZO and CeO₂ reflections. An alternative simple Raman spectroscopy analysis of crystalline quality of the CeO₂ films is proposed. The F_{2g} Raman mode of CeO₂ can be quantified either by using two polarization configurations (crossed or parallel) or at two different rotation angles around the normal axis (0° and 45°) to obtain information about the sample texture. The sample texture can be determined via a quality factor (referred as Raman Intensity Ratio, RIR) consisting in calculating the ratio of the integrated intensity of the CeO₂ F_{2g} mode at 0° and 45° in parallel polarization. This factor correlates with superconducting performance and can be used as an on-line non destructive method.

1. Introduction

The $\text{CeO}_2/\text{La}_2\text{Zr}_2\text{O}_7/\text{Ni}$ piled-up structure is a very promising architecture for $\text{YBa}_2\text{Cu}_3\text{O}_7$ (YBCO) coated conductors. Coated conductors developed by all-chemical routes are based on the excellent quality of lanthanum zirconate, $\text{La}_2\text{Zr}_2\text{O}_7$ (LZO), as buffer layer. Metal organic decomposition (MOD) allows the growth of LZO on Ni-based substrates in reducing atmosphere, which avoids the undesirable oxidation of the substrate. Pyrochlore LZO (Space Group Fd-3m) lattice parameters match those of YBCO ($|\epsilon_{\text{YBCO}} - \epsilon_{\text{LZO}}| / \epsilon_{\text{LZO}} = 1.05\%$), and it provides a good barrier against O_2 diffusion^{1,2}. This material filling all the characteristics for buffer layers (structural and chemical compatibility between substrate and active layer) has been already probed as a simple low cost architecture $\text{YBCO}_{\text{MOCVD}}/\text{LZO}_{\text{MOD}}/\text{NiW}_{\text{RABiTS}}$ ³. Nevertheless, we tried to improve the YBCO performance by adding a CeO_2 layer grown by MOCVD. The architecture YBCO (800 nm MOCVD) / CeO_2 (120 nm MOCVD) / LZO (80 nm MOD) / NiW exhibited a higher J_c value (1.2 MA/cm^2) than the one-layer buffered structure $\text{YBCO}/\text{LZO}/\text{Ni}$ ($J_c = 0.8 \text{ MA/cm}^2$).

The improvement of the YBCO properties by the addition of a CeO_2 layer has been also found by other authors⁴ concerning the CeO_2 and YBCO deposited by physical methods on LZO buffered tapes and also by Paranthaman et al⁵ with the more complex architecture YBCO (0.8 μm MOD-TFA) / CeO_2 (60 nm MOD) / LZO (200 nm MOD) / Y_2O_3 (10 nm PVD) / Ni , but with very good transport properties ($J_c = 2.5 \text{ MA/cm}^2$ and $I_c/w = 200 \text{ A/cm}$).

The main factor determining texture as well as physical properties of YBCO layer is the epitaxial and crystalline quality of the CeO_2 layer. However, the quality of CeO_2

films in the CeO₂/LZO/Ni architecture cannot be evaluated by conventional X-ray Diffraction method due to very similar lattice parameters of CeO₂ and LZO films. CeO₂ presents a fluorite structure with a lattice parameter of 5.41134 Å, while LZO crystallizes either in pyrochlore structure with a lattice parameter of 10.808 Å or in a disorder fluorite structure with a half value of the lattice parameter (5.407 Å).

In this paper we propose a simple and non-destructive Raman study of the texture quality of CeO₂ films based on the variation with polarization of the intensity of the CeO₂ F_{2g} mode in polarized spectra. The ability of Raman spectroscopy to analyse the in-plane texture of YBCO thin films has been reported since a long time⁶⁻⁹. We show that the texture quality of the CeO₂ layer can be determined by the intensity variation of the first order F_{2g} mode with polarization

2. Experimental

Ni-5%at.W RABiTS tapes presenting a cubic texture were provided by Evico GmbH (Dresden) and described previously¹⁰. The full width at half maximum (FWHM) values of the ϕ -scan (111) reflection (in plane texture) is $6^\circ \pm 0.5^\circ$, and the FWHM values of the rocking curve (ω , out-of -plane) of the (002) reflection in the longitudinal (RD) and transverse (TD) direction with respect to the rolling direction are $5.5^\circ \pm 0.3^\circ$ and $9^\circ \pm 0.3^\circ$ respectively. RABiTs tapes also present a small roughness (mean square roughness, rms < 5 nm). The grain size of the substrate is around 50 μm and its thickness is 150 μm . (001) oriented LaAlO₃ (LAO) pseudocubic single crystals provided by Crystec were also used as substrates.

Lanthanum zirconate (LZO) was grown on nickel or LAO substrates by MOD according to a procedure previously described¹¹. Lanthanum (III) 2, 4-pentadionate and zirconium (IV) 2, 4-pentadionate were dissolved in propionic acid (CH₃-CH₂-COOH) to form lanthanum and zirconium propionates. Propionic acid was added to get a total concentration of cations of 0.6 mol/l. Before deposition, substrates were ultrasonically cleaned in ethanol and acetone during 10 min. LZO films were deposited by dip coating at room temperature in a glove-box. Substrates were immersed for 30 s in the solution and withdrawn at the rate of 6 cm/min. The samples were dried at 80°C under infrared lamps for 60 s inside the glove box. The films were then annealed at 960°C under Ar + 5% H₂ gas flow for 30 min.

CeO₂ and YBCO layers were deposited by pulsed injection MOCVD on the LZO buffered Ni tape or LAO single crystal. A single liquid source based on flash evaporation using pulsed injection CVD was used to evaporate the solution. A detailed description of the deposition conditions has been already published³. The injector sequentially delivered precise micro-doses of metalorganic precursors dissolved in organic solvent: Ce(tmhd)₄ in monoglyme, or a mixture of Y(tmhd)₃, Ba(tmhd)₂, Cu(tmhd)₂ (tmhd = 2,2,6,6-tetramethyl-3,5-heptanedionate) in monoglyme with the appropriate molar ratio. The flash evaporation of the solution was performed at 280°C and film deposition took place at 750°C for CeO₂ and at 800°C for YBCO under a controlled atmosphere (60% Ar + 40% O₂) at 5 Torr of total pressure. CeO₂ layers were deposited with thickness ranging between 30 and 200 nm; YBCO thickness was 600 nm in all cases. The transport properties of the Ni/LZO/CeO₂/YBCO layers were evaluated by the determination of J_c and T_c values by susceptibility measurements. Then the

YBCO layer was chemically removed by dissolution in an aqueous orthophosphoric acid solution (1/10 v/v) before CeO₂ layer characterization.

Film texture and epitaxial relations among the different layers were determined by X-Ray Diffraction (XRD) in Shultz geometry using a D5000 Siemens four-circle diffractometer with monochromatic Cu K α radiation ($\lambda=0.15418$ nm).

Raman spectra were collected using a Jobin Yvon/Horiba LabRam spectrometer equipped with a liquid nitrogen cooled charge coupled device detector. Experiments were conducted in the micro-Raman mode in a backscattering geometry with a notch filter technology. Spectra were measured at room temperature in air-conditioned room and calibrated using the 520.7 cm⁻¹ silicon Raman peak.

Visible Raman scattering experiments were performed using the TE₀₀ 514.5 nm line of an Ar⁺ ion laser and a x50 long working distance (LWD) Olympus objective (numerical aperture = 0.5). The laser power was kept at ~ 5 mW at the sample surface on a spot size close to 2 μ m. The output light was dispersed on a 1800tr/mm spectrometer with notch filter cutting at ~100 cm⁻¹. In the following, backscattering VV and VH polarized Raman spectra will refer to the polarization of the analyzer parallel (V) and crossed (H) with respect to the incident polarization (V). The direction of the incident and scattered laser beams was normal to the substrate plane.

UV Raman scattering experiments were done at 266 nm wavelength produced from the fourth harmonic of a Nd:YAG laser. Acquisitions were obtained through a x40 UV OFR objective and with an UV extended spectrometer with 2400 tr/mm grating. The notch filter cuts at ~350 cm⁻¹ and no analyzer was used.

3. Results

LZO layers (~ 80 nm thick) were obtained by MOD on LAO single crystal and on Ni substrates. As already reported³, XRD analyses confirm the biaxial texture of the sample. For LZO layers deposited on LAO, the in-plane texture quantified from ϕ -scans performed on the (222) reflection was FWHM= 1° and the out-of-plane texture quantified from rocking curves measured on the (002) reflection was FWHM= 0.7° . On Ni-based substrates, LZO out-of-plane orientation was given by FWHM_{RD}= $5.3^\circ \pm 0.2^\circ$ in the rolling direction, FWHM_{TD}= $8^\circ \pm 0.3^\circ$ in the transverse direction and the in-plane texture was such that FWHM= $7^\circ \pm 0.3$. These results confirm that LZO grains have a c-axis orientation and that the LZO film nucleates with a biaxial texture over the substrate with its unit cell axis rotated by 45° with respect to the substrate in both cases (Figure 1).

CeO₂ grows epitaxially on LZO, with a cube-on-cube configuration. By XRD, the crystalline quality of the CeO₂ layer can be only quantified by the comparison of the intensity (counts/sec) of the (400) X-ray reflection for the same sample before and after CeO₂ deposition. If the CeO₂ layer is not completely textured or polycrystalline, an additional (222) reflection will be detected at theoretical position of $2\theta=28.6^\circ$ when using λ_{Cu} . In the case of partial crystallisation or amorphous state of the CeO₂ layer, no increase of the intensity of the (400) reflection will be measured after deposition.

In any case, the systematic measurements of the intensity before and after CeO₂ deposition are not compatible with sequential experiments and increase the delay in production of samples. As a consequence, an alternative method is needed to evaluate the texture quality of the CeO₂ layer. We will expose now the main principles involved in the Raman characterization of these buffer layers.

3.1 Raman selection rules for LZO and CeO₂ and texture evaluation

Raman spectra of LZO crystallized in the pyrochlore structure (space group Fd-3m or O_h⁷) have been reported by Vandenborre¹² as well as their mode assignment.

CeO₂ presents a fluorite structure lattice (space group Fm-3m or O_h⁵). Its first-order Raman spectrum is very simple and consists of a triply degenerated F_{2g} mode at 465 cm⁻¹, assigned to the symmetrical Ce-O stretching mode. The second order Raman spectrum is more complex and has been reported by Weber¹³.

The observation of Raman modes strongly depends on polarization selection rules. Considering the polarization directions of the incident and scattered beams, e_i and e_s , respectively, the intensity of the Raman peak F_{2g} is given by [9]:

$$I_{F_{2g}} \propto \sum_{\gamma=X,Y,Z} |e_i \cdot R(F_{2g}, \gamma) \cdot e_s|^2 \quad (1.1)$$

where $R(F_{2g}, \gamma)$ is the Raman polarizability tensor defined in the cubic crystallographic coordinate system (X=[100], Y=[010], Z=[001]) as:

$$F_{2g}(x) = \begin{pmatrix} \cdot & \cdot & \cdot \\ \cdot & \cdot & d \\ \cdot & d & \cdot \end{pmatrix} \quad F_{2g}(y) = \begin{pmatrix} \cdot & \cdot & d \\ \cdot & \cdot & \cdot \\ d & \cdot & \cdot \end{pmatrix} \quad F_{2g}(z) = \begin{pmatrix} \cdot & d & \cdot \\ d & \cdot & \cdot \\ \cdot & \cdot & \cdot \end{pmatrix} \quad (1.2)$$

From the above relations, the intensity of the F_{2g} mode in both LZO and CeO₂ crystals will be zero in the VV polarization configuration with VV = XX (or YY or ZZ) whereas it will give a Raman signal in the VH polarization configuration with VH= XY (or YZ or XZ). However, this technique has the disadvantage to depend on the efficiency of the spectrometer in VH and VV configurations.

Another way of varying the Raman intensity consists in rotating the crystal in the (X,Y) plane for a given polarization configuration. Considering the crystal oriented in

the (X,Y,Z) system with the incident beam along Z and (X,Y) the plane of incidence, θ is defined as the angle between the incident polarization V and the X crystallographic axis of CeO₂. The intensity variation of the F_{2g}(z) Raman mode present resulting from Eq. 1.1 and Eq.1.2 is given by:

$$I_{F_{2g_{VV}}}(\theta) \propto |d \sin(2\theta)|^2 \quad (1.3)$$

$$I_{F_{2g_{VH}}}(\theta) \propto |d \cos(2\theta)|^2 \quad (1.4)$$

Taking into account these equations, in a fully biaxially oriented film, a rotation of the sample around an axis normal to the substrate plane will modulate the intensity from 0 to I_{max} whereas a sample exhibiting a fibre texture or a polycrystalline sample will show no modulation at all.

3.2 Raman spectra of LZO and CeO₂

The Raman spectra of 160 nm thick MOD LZO films on Ni and on LAO did not show any detectable peak whatever the incident laser light, whereas a strong peak associated to CeO₂ peak is detectable even for very thin films (30 nm thick). We deduce that LZO presents a weak Raman scattering efficiency that is hardly detectable in our thin films. As a consequence, Raman spectroscopy cannot be used to evaluate LZO texture quality and the Raman spectrum of the CeO₂/LZO structure did not differ from the CeO₂ film spectrum.

We also studied the CeO₂/LZO/Ni heterostructure by UV Raman scattering. The excitation at 266 nm (above the optical gap of CeO₂ at 3.2 eV) results in a strong absorption of light at the CeO₂ surface. The visible and UV Raman spectra confirms that the Raman intensity result mainly from the CeO₂ layer. Nevertheless, these spectra show some differences: the CeO₂ film Raman spectrum obtained with Ar⁺ laser light involved a single Raman line at 465 cm⁻¹ related to the CeO₂F_{2g} mode (Figure 2). When

using UV excitation, higher frequency bands near 600 and 1180 cm^{-1} were also collected in addition to the F_{2g} mode. They were assigned to second-order features of CeO_2 excited by the UV laser light (Figure 2). In the following, we will focus on the F_{2g} mode measured with Ar^+ laser excitation.

The CeO_2/LZO structure (Figure 3) grows biaxially textured on a nickel cubic substrate and on (001) LAO, but rotated by 45° . We will define a new reference system (X,Y,Z) made of the geometrical axis of the sample with $Z=z$ normal to the surface and (X,Y) in coincidence with the [100] and [010] directions of the LAO or Ni substrate. On the other hand, the reference system (X', Y') for the definition of the Raman tensor taking into account the CeO_2 crystal axis used in Eq. (1.2) is rotated by 45° on the (X, Y) reference system. We will define the rotation angle α_s around the normal Z in the (X,Y,Z) system to be 0° (Figure 2a) in the [100] direction of the LAO substrate or the Ni tape. The rotation angle α_s and the θ angle defined in Eq. (1.3) and Eq. (1.4) are related as follows: $\alpha_s = \theta + 45^\circ$. This means the F_{2g} mode is Raman active in the parallel configuration (VV) at 0° rotation angle.

The equivalence between both experimental configurations can be observed for a $\text{CeO}_2\text{-MOCVD}$ (30nm)/ LZO-MOD (80 nm)/ Ni structure as shown in Figure 4. First, spectra were collected at $\alpha_s = 45^\circ$, i.e. in the CeO_2 crystal reference system, to obtain the standard variation of the F_{2g} mode with polarization (Figure 4a). The intensity of VH spectrum was corrected from the spectrometer efficiency by increasing the acquisition time (x3) in comparison with VV spectrum. The highest CeO_2 F_{2g} mode intensity was obtained in VH spectra for $\alpha_s = 45^\circ$ (equivalent to VV $\alpha_s = 0^\circ$) and decreases in VV spectra for $\alpha_s = 45^\circ$. Then (Figure 4b), spectra were measured in VV polarisation configuration for two rotation angles: at $\alpha_s = 0^\circ$ and at $\alpha_s = 45^\circ$. The highest CeO_2 F_{2g}

mode intensity was obtained in VV spectra for $\alpha_s = 0^\circ$. Both series of measurements give evidence that spectra obtained in VV polarisation at 0° and at 45° contain the same texture information than spectra issued from a change in polarisation configuration, but it is a faster and more direct method.

Some additional Raman modes are also observed in this spectrum. As suggested by the reference spectrum of nickel oxide obtained by thermal oxidation of a nickel substrate in air at 800°C for 5min, they have been identified as NiO modes due to the nickel oxidation through the LZO layer during the MOCVD process.

3.3 Angular dependence of CeO_2 F_{2g} Raman intensity

The dependence of the intensity of the CeO_2 F_{2g} mode in a $\text{CeO}_2/\text{LZO}/\text{LAO}$ sample has been studied by varying α_s in VV polarization configuration. For this experiment, we have used a CeO_2 layer deposited on LZO-buffered LAO instead of Ni substrate to avoid the NiO signal in the spectrum. Both spectra shown in Figure 5 for $\alpha_s=0^\circ$ and $\alpha_s=45^\circ$ correspond to the highest intensity variation. The peak observed at 462 cm^{-1} is related to the CeO_2 F_{2g} mode whereas the 500 cm^{-1} one corresponds to the E_g mode of LAO [14]. Both modes are Raman active in VH configuration, but they appear out of phase due to the 45° rotation between the LAO and CeO_2 lattices.

The modulation of the CeO_2 F_{2g} mode intensity with the rotation angle, α_s , has been determined by measuring four points at each angle to estimate the dispersion. Peaks were fitted and the integrated intensities thus obtained are reported in Figure 6. The intensity variation with α_s follows a cosinus law (or a sinus with θ) as predicted by Eq. (1.3)

3.4 Raman Intensity Ratio and YBCO performances

To determine the correlation of the CeO₂ layer texture with the intensity ratio of the F_{2g} Raman mode at 0° and 45°, we have defined a Raman Intensity Ratio (RIR) given by the integrated intensity ratio of CeO₂ F_{2g} Raman mode at 0° and 45° in VV polarization (RIR= $I_{VV}(0^\circ) / I_{VV}(45^\circ)$). We have studied the correlation of YBCO performance (J_c values) for several YBCO/CeO₂/LZO samples on Ni and on LAO with RIR. The quality of the YBCO layer was not identical in all the samples, so the J_c values are strongly dependent on the experiment. Results are summarized in Table I as well as FWHM values obtained from XRD characterizations. A correlation diagram between the RIR and J_c values is presented in Figure 7 for each sample. It is to be noticed that the number included in the sample label denotes the YBCO deposition experiment; so V19Ni and V19LAO are related to the same YBCO deposition but on two different substrates: the poor J_c value obtained with the LAO sample, correlated to an absence of texture in YBCO film, can be only explained by a poorly textured CeO₂ layer. This is characterized by a RIR value smaller than 1. On the other hand, the highest J_c values were obtained for samples with RIR values higher than 2.5.

4. Discussion

Raman studies performed on CeO₂ layers have indicated that information about the film texture can be easily obtained from the F_{2g} Raman mode. This mode does not overlap with other Raman modes coming from the different materials used in the coated conductor architecture and its intensity is very high, even for very thin films (30 nm thick CeO₂, Figure 4). It has also been shown that the biaxial texture of this layer gives

an intensity modulation of the F_{2g} Raman mode when rotating the sample around an axis normal to the substrate plane; this modulation is not thickness dependent.

Raman spectra obtained in VV polarization configuration at 0° and at 45° rotation angles allow to detect a modulation in the CeO_2 F_{2g} mode intensity due to the film texture. The calculation of the intensity ratio from both spectra allowed to define a quality factor RIR. RIR values higher than 1 attests the biaxial texture of the CeO_2 layer. Otherwise, the buffer layer is poorly or not textured and will not transmit the texture template to the YBCO layer. The CeO_2 crystalline quality depends on the crystalline quality of the LZO surface. Indeed, despite a well-textured structure revealed by the (00 l) reflections in their XRD pattern, some LZO layers did not offer a sufficiently high crystalline quality of their surface to obtain a well crystalline contrast in EBSD or by RHEED analyses. Unfortunately, last techniques cannot be routinely used in coated conductor fabrication to qualify the substrates. When using LZO layers as template in next steps, i.e. CeO_2 deposition and YBCO deposition, XRD diagrams are no more accurate enough to evaluate the crystalline quality of the CeO_2 layer while the RIR estimation can give this information before YBCO deposition. Thus, this quality factor can be very useful to qualify substrates for YBCO deposition during the fabrication process.

The collection of the Raman data was performed with using a large working distance x50 objective, which allows the analysis into a small spot ($\sim 2 \mu\text{m}$) at a relatively long distance from the sample ($\sim 2 \text{cm}$). On the other hand, this analysis is non destructive, rapid and extremely local. It can be performed without sample preparation, at atmospheric pressure, directly or through a quartz window on any substrate shape. All these features indicate that Raman characterization of CeO_2 layer can be used to control

the sample quality in an on-line process or to perform selective tests on sample uniformity.

5. Conclusions

Raman spectroscopy has been used to characterize CeO₂/LZO structures with different CeO₂ thicknesses. We have shown that the F_{2g} Raman mode of CeO₂ can be quantified from spectra collected either in two polarization configurations (VV and VH) or at two rotation angles around an axis perpendicular to the substrate plane (0° and 45°) in VV polarization configuration to obtain information about the sample texture. This kind of information cannot be obtained from XRD measurements due to the overlap of the LZO and CeO₂ lattices. We have defined a quality factor (RIR) consisting in the calculation of the intensity ratio of the CeO₂ F_{2g} mode at 0° and 45° in VV polarization. The RIR value quantifies the intensity modulation between both configurations. We have correlated this factor to superconducting performances (J_c). RIR should be higher than 1 to ensure a crystalline quality of the CeO₂ layer sufficiently high to template the YBCO layer. This determination is fast, non destructive and compatible with an on-line characterization during the fabrication of coated conductors.

Acknowledgement

This work has been financially supported by the French Research National Agency (ANR) through the MADISUP Project and by Région Rhône-Alpes SESUC project. We acknowledge Dr Ph. Odier (Institut Louis Néel – CRETA) for fruitful discussions and Dr. M. Decroux (Geneve University) for the collaboration in the J_c measurements.

References

1. W. Seo, J. Fompeyrine, A. Guiller, G. Norga, C. Marchiori, H. Siegwart, J.P. Locquet. *Appl Phys Lett* **83**, NO 25, 5211 (2003).
2. K. Knoth, R. Hühne, S. Oswald, L. Schultz, B. Holzapfel, *Acta Mater*, **55**(2) 517, (2006).
3. T. Caroff, S Morlens, A Abrutis, M Decroux, P Chaudouët, L Porcar, Z Saltyte, C Jiménez, P.Odier and F Weiss. *Supercond. Sci. Technol.* **21**, 075007, (2008)
4. K. Knoth, R. Hühne, S. Oswald, L. Molina, O. Eibl, L. Schultz, B. Holzapfel. *Thin Solid Films* **516**, 2099, (2008).
5. M.P. Paranthaman, S. Sathyamurthy, M.SZ. Bhuiyan, P.M. Martin, T. Aytug, K. Kim, M. Fayek, K.J. Leonard, J. Li, A. Goyal, T. Kodenkandath, W. Li, W. Zhang, M.W. Rupich, *IEEE Trans. on Appl. Supercond.* Vol **17** No 2, 3332, (2007).
6. J.C. González, N. Mestres, T. Puig, J. Gázquez, F. Sandiumenge, X. Obradors, A. Usoskin, Ch. Jooss; H.C. Freyhardt, R. Feenstra. *Physical Review B*, **70**, 094525, (2004)
7. U. Weimer, R. Feile, P. Leiderer, U. Poppe, J. Schubert, J. Fröhlingdorf, B. Stritzker, W. Zander. *Physica C* **168**, 359, (1990)
8. N. Diekmann, R. Kürsten, M. Löhndorf, A. Bock. *Physica C* **245**, 212, (1995).
9. C. Thomsen, R. Wegerer, H.-U. Habermeier, M. Cardona. *Solid State Comm.* Vol **83**, No. 3, 199, (1992).

10. J. Eickemeyer, D. Selbmann, R. Opitz, B. De Boer, B. Holzapfel, L. Shultz, U. Miller Supercond. Sci. Technol. **14** 152, (2001).
11. Z.M. Yu, P. Odier, L. Ortega, L. Zhou, P.X. Zhang, A. Girard Materials Science and Engineering B **130** 126, (2006).
12. N.T. Vandenborre, E. Husson, H. Brusset. Spectrochimica Acta, Vol **37A**, 113, (1981).
13. W.H. Weber, K.C. Hass, J.R. McBride. Physical Review B Vol **48**, N 1, 178, (1993).
14. J.F. Scott. Physical Review Vol **183**, NO 3, 823, (1969).

Sample	RIR	YBCO texture: in plane and out of plane FWHM (°)			J_c (MA.cm ⁻²)	CeO ₂ thickness (nm)
		(103) _φ	(005) _{ω_{RD}}	(005) _{ω_{TD}}		
		V13LAO	33	1.5°		
V13Ni	3.3	8.7°	5°	7.1°	0.1	30
V15LAO	9.6	1.6°	0.55°		0.5	150
V15Ni	1.33	-	-	-	0.07	150
V17LAO	1.6	-	-	-	0	200
V17Ni	2.6	8.2°	5.2°	6.7°	0.5	200
V19LAO	0.88	Non-textured	1°		0	60
V19Ni	3.8	7.9°	5.5°	7.5°	0.25	60
V21Ni	5.85	7.7°	5.2°	7.4°	1.2	120
V23Ni	2.6	7.9°	5.3°	7.8°	0.2	60

Figures

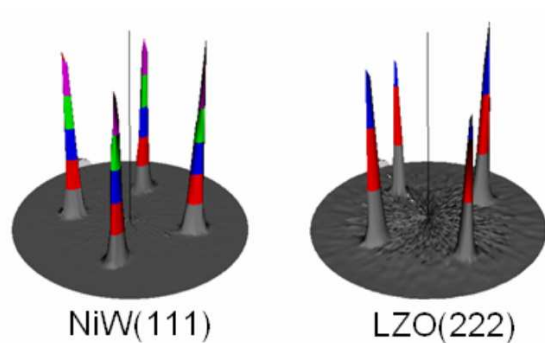


Figure 1: Ni and LZO pole figures obtained by XRD on a LZO/Ni sample

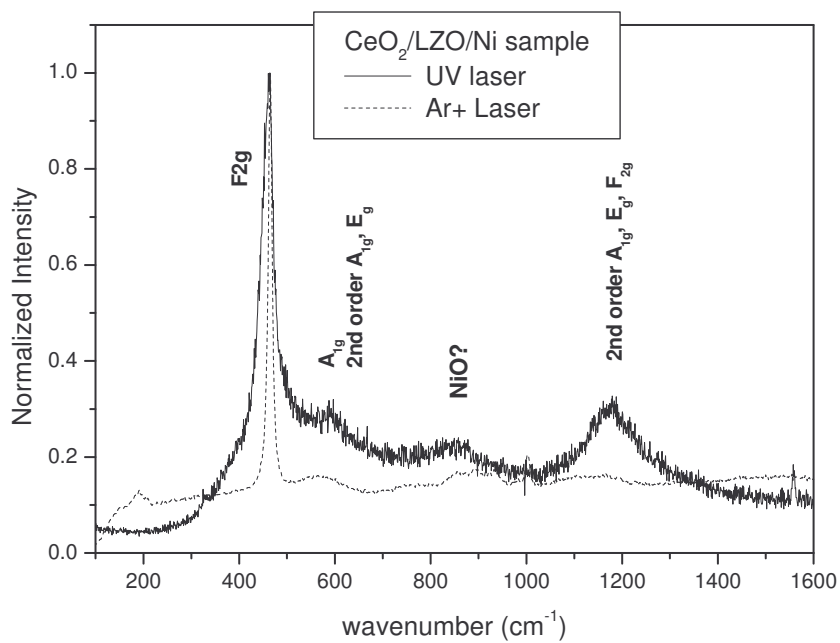


Figure 2: Raman spectra of a CeO_2 layer on LZO/Ni obtained with a UV laser (continuous line) or an Ar^+ laser (dashed line). Labelled modes are related to CeO_2

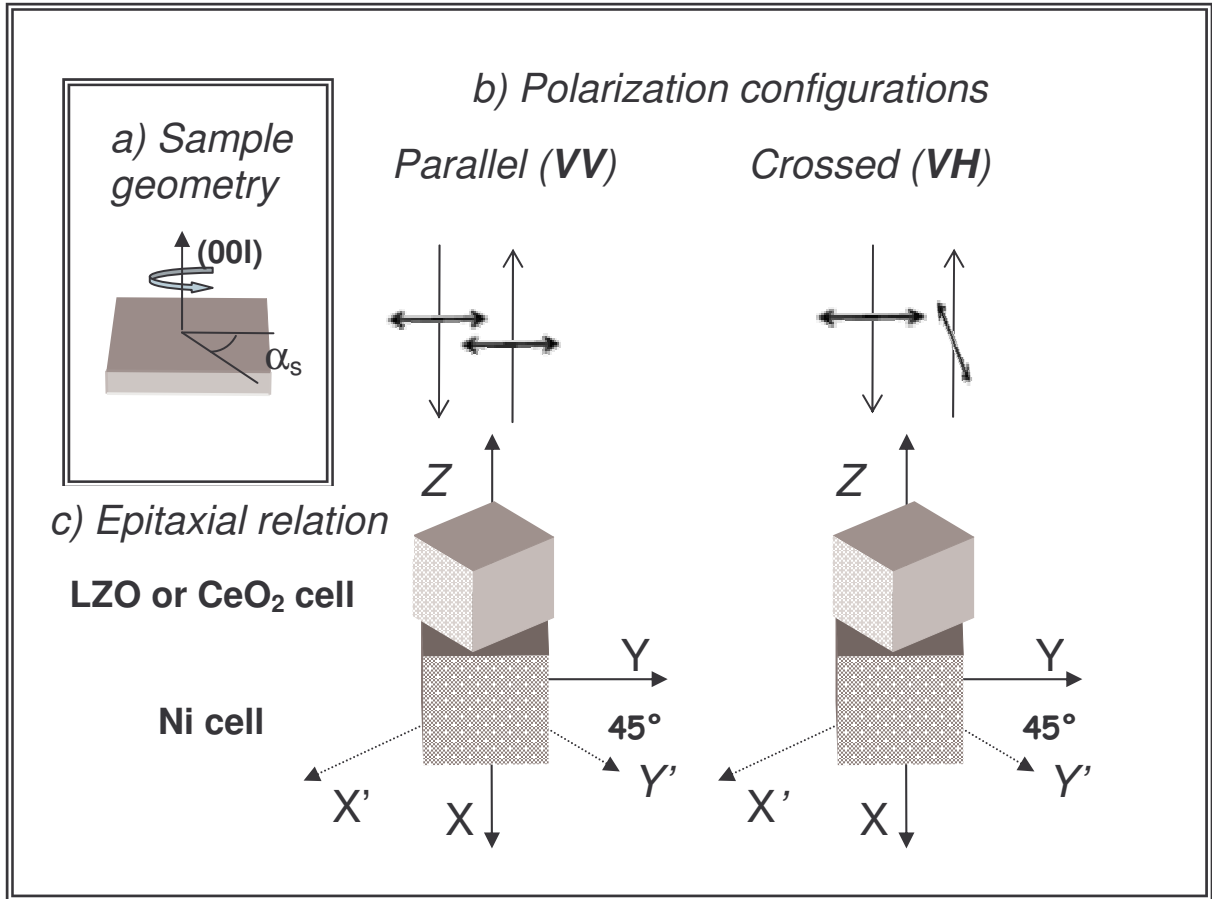


Figure 3: Schematic representation of the experimental setup.

- a) Description of the α_s angle used for intensity modulation, which defines the rotation of the sample around its normal.
- b) Polarization configurations in the (X,Y,Z)sample reference system.
- c) Representation of the crystal cell of LZO or CeO₂ rotated by 45°with respect to the Ni cell.

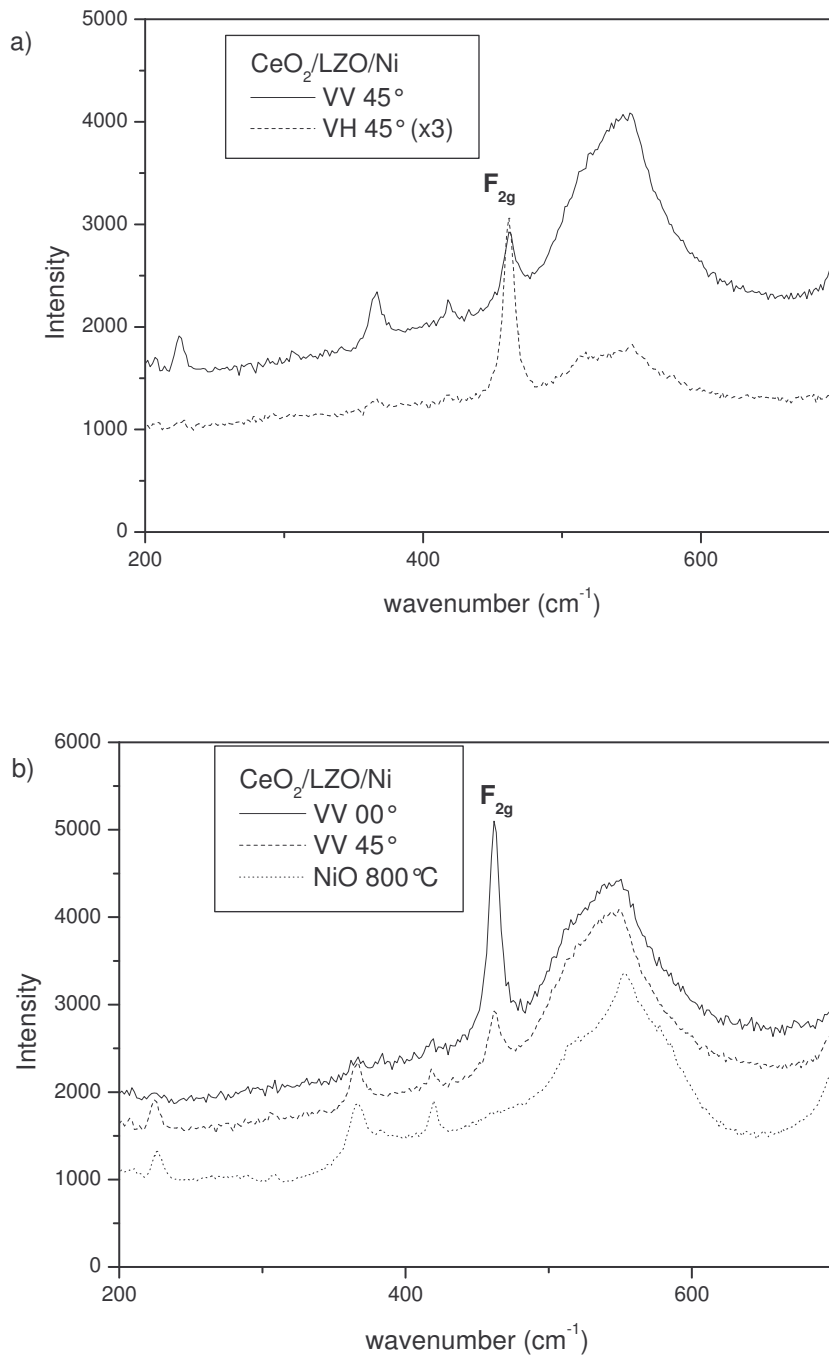


Figure 4: Raman spectra of a 30 nm thick CeO_2 layer on LZO/Ni.

a) In the CeO_2 crystal axis reference system ($\alpha_s=45^\circ$) using VV (solid line) and VH polarization configurations (dashed line, acquisition time x3).

b) In VV polarisation configuration at $\alpha_s=0^\circ$, (i.e. in the substrate reference system, solid line) and at $\alpha_s=45^\circ$ (i.e. in the CeO_2 crystal reference system, dashed line). The Raman spectrum of a thermal NiO film obtained by direct oxidation of Ni tapes at 800°C is also presented (dotted line).

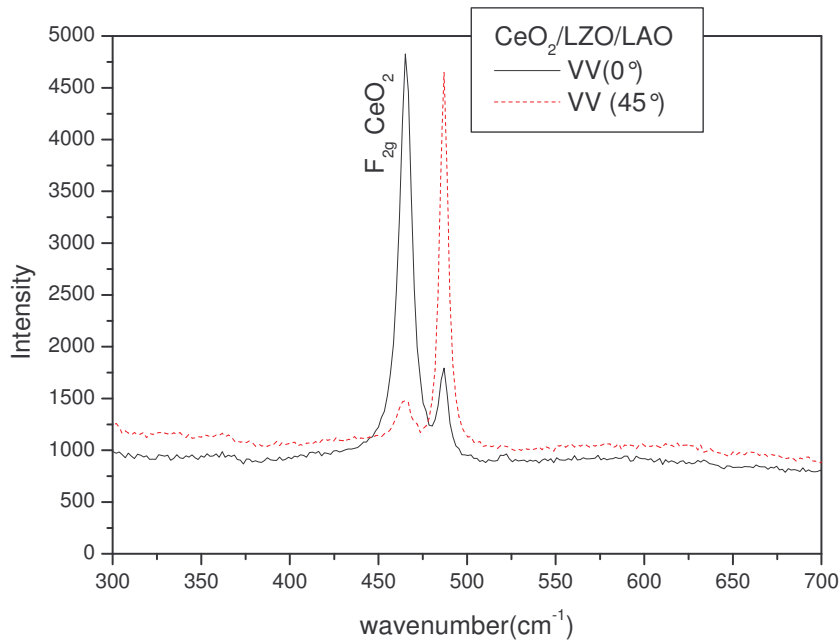


Figure 5: Raman spectra of a CeO_2 layer on LZO/LAO. The peak near 500 cm^{-1} is related to LAO E_g mode.

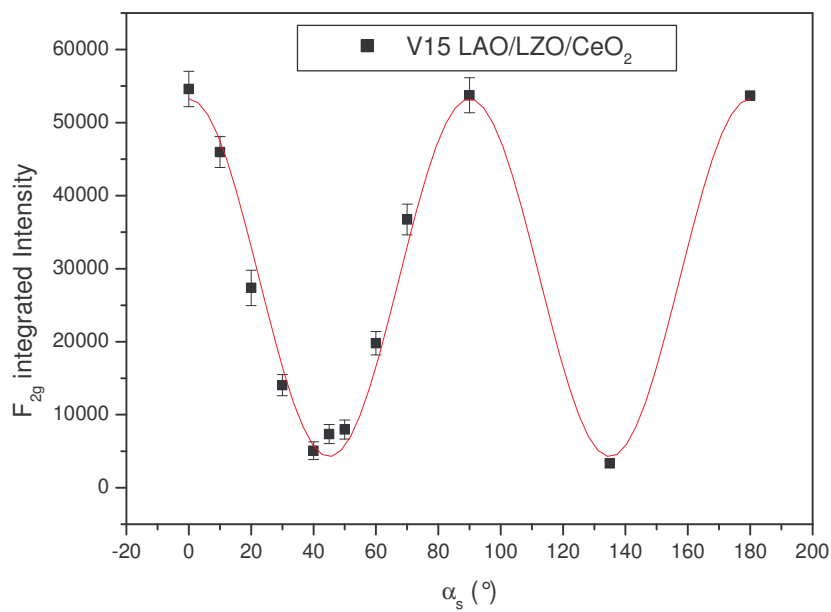


Figure 6:

Intensity modulation of the F_{2g} Raman mode of CeO_2 (465 cm^{-1}) in a $CeO_2/LZO/LAO$ structure measured in VV polarization configuration.

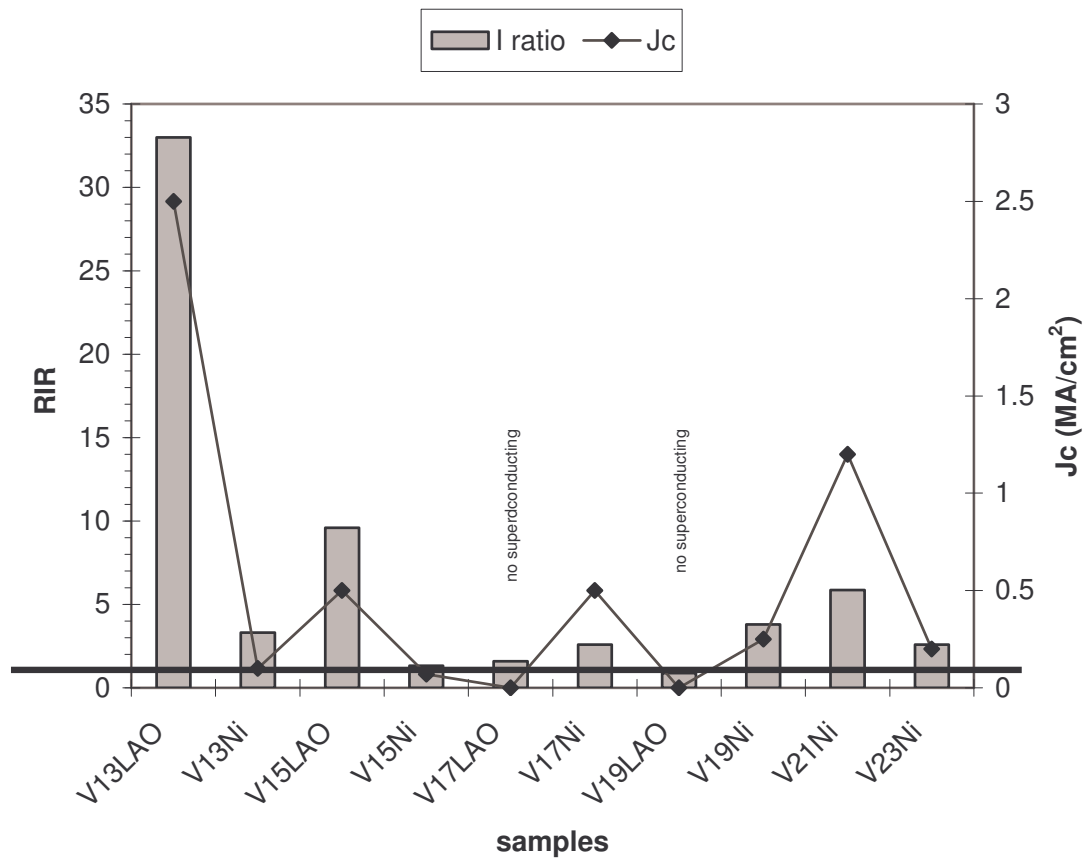


Figure 7: Correlation diagram between RIR ($=I(0^\circ) / I(45^\circ)$) and J_c values measured in samples consisting in YBCO/CeO₂/LZO structure. The sample name is relative to the substrate used and the experiment number for YBCO deposition.